REPORT DOCUMENTATION PAGE

Form Approved

OMB No. 0704-0188

1. AGENCY USE ONLY (Leave Blank)	2. REPORT DATE	3. REPORT TYPE AND DATES COVERED
	29 July 2005	Final (4/15/03 – 4/14/05)

4. TITLE AND SUBTITLE
SAS Imaging and the Sea Surface Bounce Path

5. FUNDING NUMBERS
N00014-03-1-0635

6. AUTHOR(S)
Peter H. Dahl

7. PERFORMING ORGANIZATION NAME(S) AND ADDRESS(ES)
Applied Physics Laboratory
University of Washington
1013 NE 40th St.
Seattle, WA 98105-6698

8. PERFORMING ORGANIZATION REPORT NUMBER

9. SPONSORING/MONITORING AGENCY NAME(S) AND ADDRESS(ES)
Office of Naval Research
One Liberty Center
875 North Randolph St., Ste. 1425
Arlington, VA 22203-1995
Attn: Dr. Kerry Commander, Code 32MS

10. SPONSORING/MONITORING AGENCY REPORT NUMBER

11. SUPPLEMENTARY NOTES

12a. DISTRIBUTION/AVAILABILITY STATEMENT
Approved for public release

12b. DISTRIBUTION CODE

13. ABSTRACT (Maximum 200 words)

Modeling and interpretation of SAS measurements taken during SAX04 experiment in conducted near Panama City, Florida (fall 2004), is completed. Both data and simulation show how multipath interaction with the sea surface delivers the SAS transmit waveform roundtrip, and causes three time horizons for a single target located near the sea surface. The results shed light on the role of sea surface interaction in SAS methodologies whenever they are applied to: (1) long-range applications, e.g., over-the-horizon SAS (OTHSAS), or SAS Systems at Far Ranges and Severe Sites (SASSAFRASS); and (2) applications involving detection and imaging of near-surface targets.

14. SUBJECT TERMS
Synthetic Aperture Sonar (SAS), sea surface interaction, multipath, bistatic scattering

15. NUMBER OF PAGES
13

16. PRICE CODE

17. SECURITY CLASSIFICATION OF REPORT	18. SECURITY CLASSIFICATION OF THIS PAGE	19. SECURITY CLASSIFICATION OF ABSTRACT	20. LIMITATION OF ABSTRACT
Unclassified	Unclassified	Unclassified	UL

29 July 2005

FINAL REPORT

SAS Imaging and the Sea Surface Bounce Path

ONR Grant N00014-03-1-0635

Peter H. Dahl,

Applied Physics Laboratory, University of Washington

EXECUTIVE SUMMARY

The research is geared towards evaluating the performance envelope of long-range SAS when sea surface forward scattering and reflection is utilized as the propagation channel. The final results focus on modeling and interpretation of SAS measurements taken during the SAX04 experiment conducted near Panama City, Florida (fall 2004), during which images of near-surface target at range ~35 m were made.

The key results are as follows:

1. A simulation code (Matlab) was developed to evaluate multipath interaction with the sea surface in SAS imaging of a near-surface target.
2. Both data and simulation show:
   a. Four paths deliver the transmit waveform roundtrip, one being the direct path to and from the target, and other three involve interaction with the sea surface. The result is three time horizons, or SAS "smiles", originating from the near-surface target (because two paths are equal-time).
   b. The middle time horizon is the most energetic owing to the contribution of two paths.
   c. The middle and third time horizon *do not* focus in SAS processing owing to interaction with the sea surface.
3. The results shed light on how sea surface interaction plays a role in SAS methodologies whenever they are applied to: (1) long-range applications, e.g., over-the-horizon SAS (OTHSAS), or SAS Systems at Far Ranges and Severe Sites (SASSAFRASS), and (2) applications involving detection and imaging of near-surface targets.

For the "long range" application the sea surface forward scattering coherence time, τ^*, cannot be exceeded, if focusing of paths involving the sea surface is desired.

For the "near-surface targets" application the same applies. However, it is also advantageous to use SAS measurement parameters that deliberately exceed τ^*, in order to filter out multipaths involving the sea surface. This results in better resolution and removal of spurious "ghost" images, which is useful for swimmer detection and other port security imaging tasks.

1. INTRODUCTION

This report summarizes final results of a grant entitled Simulating Long-Range SAS Imaging via the Sea Surface Bounce Path, (ONR Grant # N00014-03-1-0635). The research was geared towards evaluating the performance envelope of long-range SAS when sea surface forward scattering and reflection is utilized as the propagation channel, and also more broad utilization of the sea surface path in SAS applications.

Incremental progress has been reported in ONR annual reports for FY03 and FY04. Results reported in this final report were partially completed in FY05 (owing to the timing of the grant) and involve modeling and interpretation of SAS measurements taken during SAX 04. These measurements involve SAS processing of a near-surface target at range 35 m.

2. SAX 04 SYNTHETIC APERTURE SONAR (SAS) RAIL STUDY OF A NEAR-SURFACE TARGET

The synthetic aperture sonar (SAS) measurements were conducted on October 27, 2004 (approximately 1400 local time), by Kevin Williams of APL-UW, as part of SAX04, using the APL-UW experimental SAS rail system [1]. The SAS source/receiver array was translated horizontally 25.6 m (Fig. 1) at rate 5 cm/s, with sonar pulse transmitted and subsequent reverberation recorded for every 2.5 cm of translation, equivalent to a pulse repetition period of 0.5 seconds. The pulse was a linear FM sweep of duration 4 ms, frequency range 6 to 10 kHz. A spherical target float (diameter ~25 cm) was placed at depth 2 m, such that range to the source/receiver array would be minimized upon the SAS rail system translating 20 m.

The transmit beam aperture was 20 cm by 20 cm, and the receive aperture was 10 cm (horizontal) by 20 cm (vertical), which are qualitatively represented in Fig. 1. Both apertures had their primary axes oriented horizontally, and for this analysis the received data were beam-formed using the vertical aperture to an equivalent 15° upward pitch, in order to isolate returns originating from the region near the sea surface. Matched filtering of the beam-formed raw data (Fig. 2) shows three parallel event horizons, in the classic "smile" form, with shortest range occurring at about ping 800 as expected. (The other, weaker, event horizons visible in Fig. 2 likely originate from the tether and bottom

mooring hardware associated with the surface target, since the beam forming cannot perfectly eliminate these returns.) The "smile" fades near the start of the run (pings 1 to ~300) owing to 2-way beam pattern modulation.

The three parallel event horizons originate from multipath interaction with the sea surface as diagrammed in the lower part of Fig. 2. The nature of such interaction has been studied in the context of reverberation from near-surface bubbles [2], and it is interesting to observe it in this application.

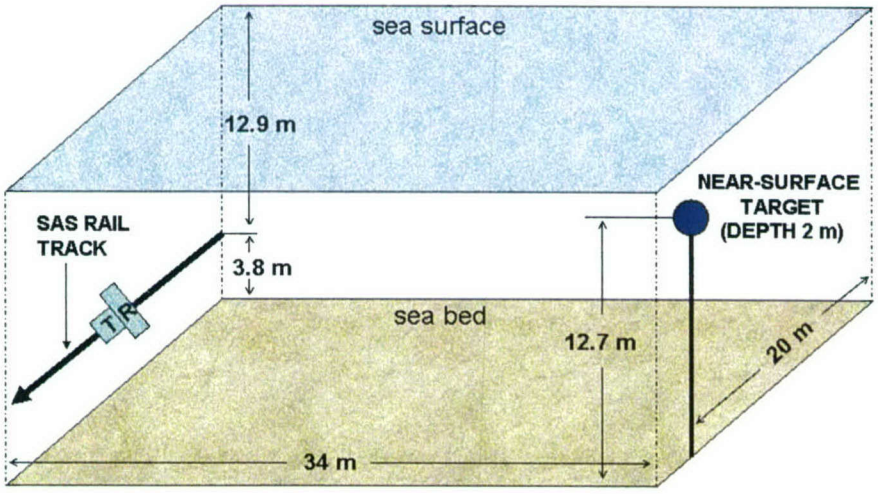

Figure 1. Approximate geometry for SAS near-surface target study. The APL-UW SAS rail starts translation in upper left corner; the transmit (**T**) - receive (**R**) array moves along the direction of thick arrow at rate 2.5 cm/s, during which there is a sonar ping every 5 s. The initial slant range to target is ~40 m; at ping ~800 the horizontal range is minimized (~34 m) and slant range is ~35 m. Translation ends at ping 1024 for total of 25.6 m of translation along the rail track.

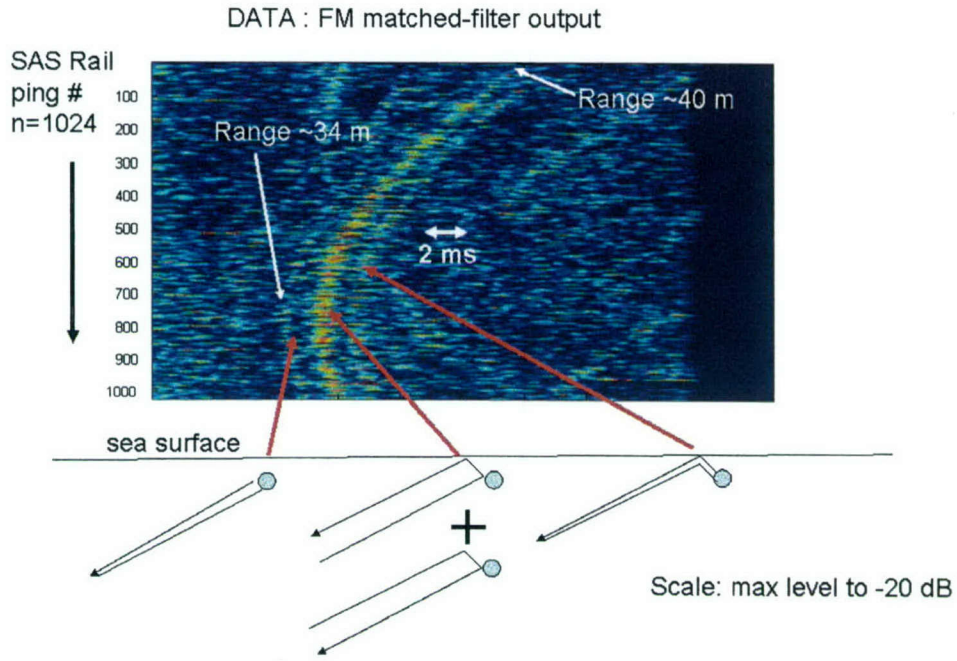

Figure 2. Matrix of matched-filtered output, equal to 20 $\log_{10}$ ($|MF\ (t;\ n)|$), where $MF(t;\ n)$ is the matched-filtered output as a function of time (horizontal axis) for the n^{th} ping (vertical axis). A 20 dB dynamic range is displayed. The rows correspond to translation along the rail track in Fig. 1, with minimum range-to-target reached at ping 800. Three primary event horizons (arrows) correspond to the four pathways (shown in diagram below data) connecting source/receiver array with the target sphere. Note: There is only one target; arrival time difference is due to the presence of the nearby sea surface boundary.

3. SIMULATION OF THE SAS RAIL MEAUSUREMENTS

The data shown in Fig. 2 were simulated as follows. A complex-valued amplitude impulse response $\boldsymbol{I_n}$ is generated for each ping number $\boldsymbol{n}$, that is intended to represent propagation to and from the target, along with bistatic scattering and near-specular reflection from the sea surface. A simulation of the "raw" data as measured in the field is obtained upon convolving $\boldsymbol{I_n}$ with the FM waveform, and adding simulated in-band noise

to match the SNR of the data. Matched filtering and SAS computations can be subsequently applied to this simulated data.

The impulse response $\boldsymbol{I_n}$ is composed of separate contributions corresponding to the paths shown below Fig. 2. First, the direct path to and from the spherical target (Fig. 2 diagram, left), is modeled by $A_n\delta(t-t_{D_n})$, where $t_{D_n}=\frac{2R_n}{c}$ with R_n equal to the slant range to the target (a function of ping number n) and c the nominal sound speed. The amplitude A_n is set equal to $\frac{1}{R_n^2}$.

Next, paths involving the sea surface (Fig. 3) are modeled using an approach similar to that discussed in [3], i.e., requiring maps of the bistatic cross section per unit area of sea surface computed for conditions corresponding to wind speed of 5 m/s and rms waveheight of 14 cm, representing the nominal conditions at the time of the measurements. New maps of bistatic scattering are generated to reflect change of geometry as the SAS rail translates along the rail track. For the two paths that interact with the sea surface one time (Fig. 3, left), there are two impulse responses. The response, $\boldsymbol{I_1}$ (Fig. 3, lower left), is computed on the assumption of a true source at the current rail position and a virtual receiver at the target. Likewise, the response, $\boldsymbol{I_2}$ (Fig. 3, upper left), is computed on the assumption of a virtual source at the target position (point source) and a true receiver at the current rail position. Both $\boldsymbol{I_1}$ and $\boldsymbol{I_2}$ are then completed by inclusion of a

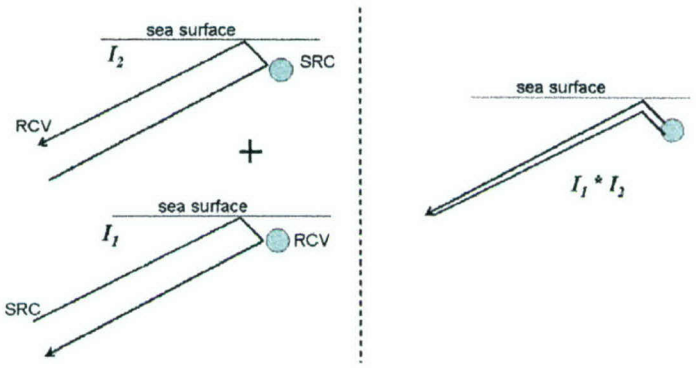

Figure 3. Paths interacting with the sea surface one time (left side of vertical dashed line), and path interacting with sea surface two times (right side).

propagation factor, to or from the spherical target, whichever applies. In addition, the appropriate beam pattern weighting is applied to mimic: (1) the source array, (2) the 15° upward tilt in the receiving array, and (3) translation of the SAS rail from ping 1 to 1032, with ping 800 corresponding to approximate boresite. Because the two versions of the single-sea-surface-interaction path, $I_1$and I_2, are reciprocal, they are coherently added together.

Note: each I_1 and I_2 computed for a *given* ping utilize the same statistically "frozen" sea surface, as the coherence time for the sea surface, $\tau^* \approx 0.3$ s, is much greater than $\frac{R_n}{c} \approx 0.025$ s. We discuss the significance of τ^* further below. However, between pings that are separated by 0.5 s, we assume an independent realization of the sea surface. To relate the complex amplitude impulse responses computed here, with the intensity impulse response computed in [3], the former must be squared and ensemble averaged over a large number of pings.

For the path that interacts with the sea surface two times (Fig. 3 right), we take I_1 (without inclusion of the additional propagation factor from the target to the receiver), along with the similar form of I_2, and convolve these to form the impulse response. This approach fully captures the additional time spreading that ensues from interacting with the sea surface twice rather than one time. Finally, the three path types are assembled into one impulse response, for which examples from two pings are shown in Fig. 4; ping 800, the ping the closest approach to the target, and ping 1, for which target is at a greater range and also not within the main lobe of the transmit beam. We obtain the simulated data (Fig. 5) upon convolving responses like this (in complex form) with the FM waveform, adding the in-band noise, and match-filtering.

The real data in Fig. 2 and synthetic data in Fig. 5 display similar arrival time horizons associated with multipath propagation to and from the near-surface target. As both model and data display random features, a better quantitative comparison is an intensity-average over a large number of pings; since the SAS rail is in motion, we limit this average (Fig. 6) to 20 pings and about certain locations.

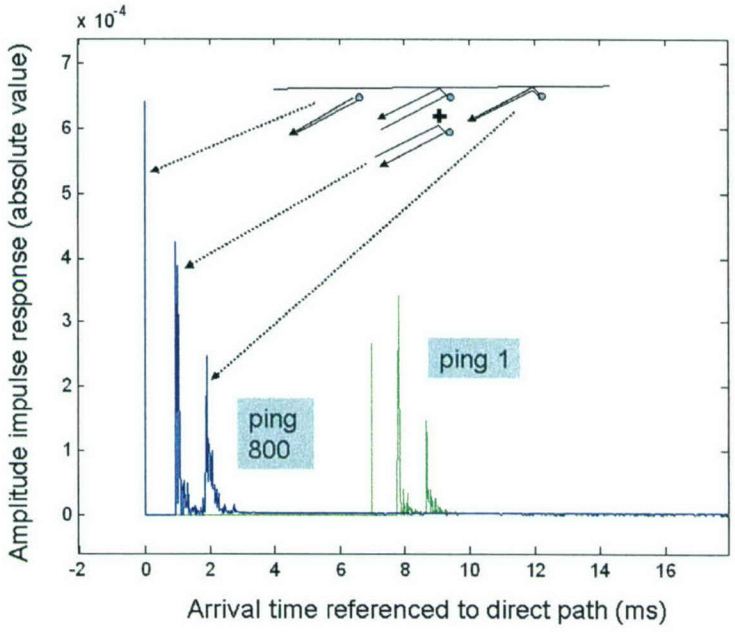

Figure 4. Amplitude of the impulse response for propagation to and from point target located 2 m below the sea surface, as a function of ping number. The impulse response has three components associated with the paths as shown. The arrival times are referenced to that of the direct path for ping 800. The impulse responses are noise-free, with in-band noise added after convolution with the transmit pulse.

From Fig. 6, both the model and simulation show that: (1) four paths deliver the FM waveform roundtrip, with 2 paths being reciprocal thus giving three time horizons, and (2) the middle time horizon is the most energetic owing to the contribution of two paths.

Figure 7 is an SAS image derived from the data shown in Fig. 2. The image displays one primary target location, and we believe the other targets are the result of stationary clutter associated with the mooring hardware that is difficult to eliminate completely through beam forming. The SAS image from the data suggests that only one time horizon produces a SAS image. *The remaining two time horizons that involve the sea surface do not enter into the SAS image owing to the de-correlating effects of the sea surface.*

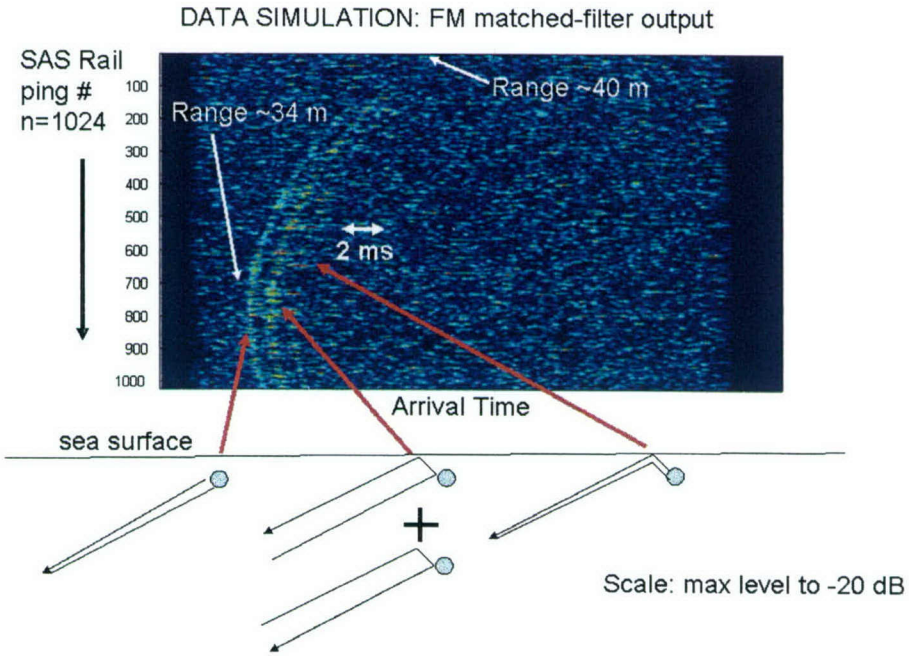

Figure 5. Simulated matrix of matched-filtered output, equal to $20 \log_{10} (|MF\ (t;\ n)|)$, where $MF(t;\ n)$ is the matched-filtered output as a function of time (horizontal axis) for the n^{th} ping (vertical axis). A 20 dB dynamic range is displayed. The rows correspond to translation along the rail track in Fig. 1, with minimum range-to-target reached at ping 800. Three primary event horizons (arrows) correspond to the four pathways (shown in diagram below data) connecting source/receiver array with the target sphere. Note: There is only one target; arrival time difference is due to the presence of the nearby sea surface boundary.

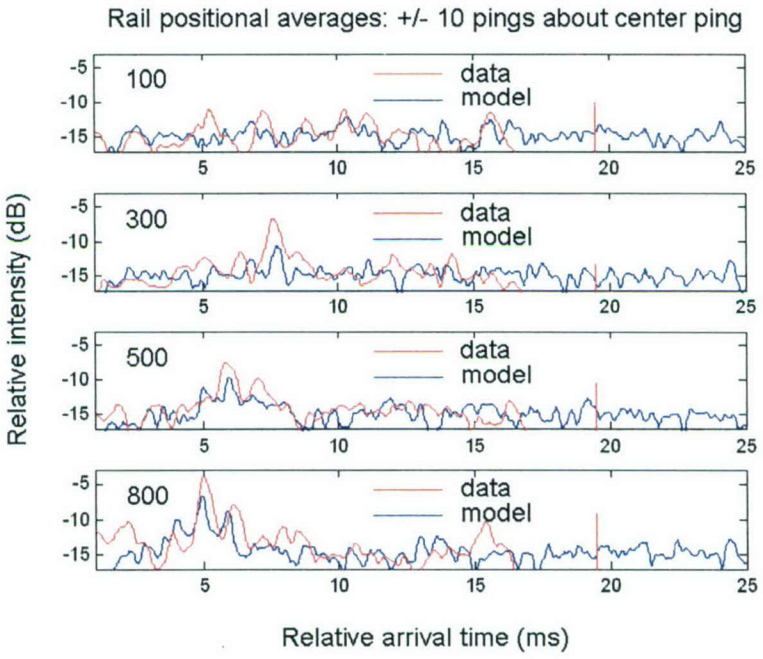

Figure 6. Intensity average of model (blue) and data (red) about four rail locations as indexed by ping number (noted on left). Vertical red line on right side is artifact, and the simulation duration is longer than data duration (~18 ms).

To test this idea, an SAS image (Fig. 8) is generated from the synthetic data shown in Fig. 5, and again the image displays only one primary target location. Furthermore, using the synthetic data we can repeat the simulation but this time excluding all paths that interact with the sea surface. *The result is the exact same image as shown in Fig. 8.*

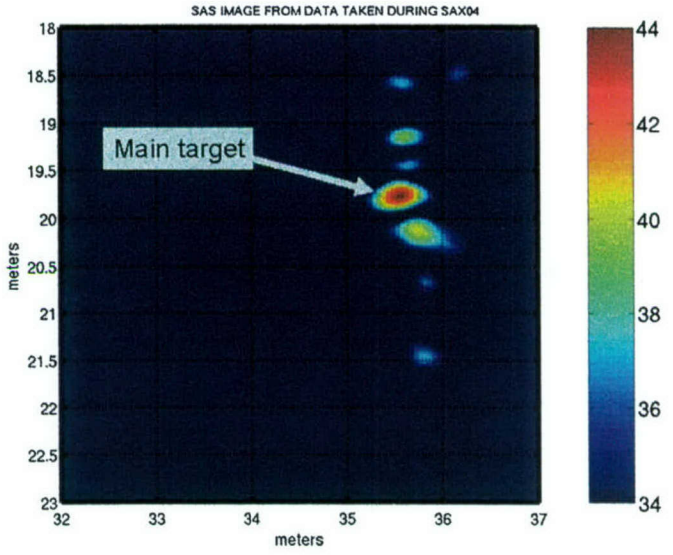

Figure 7. SAS image derived from the data shown in Fig. 2. The main target is noted by the arrow with other targets likely due to clutter associated with mooring hardware. A 10 dB dynamic range is shown.

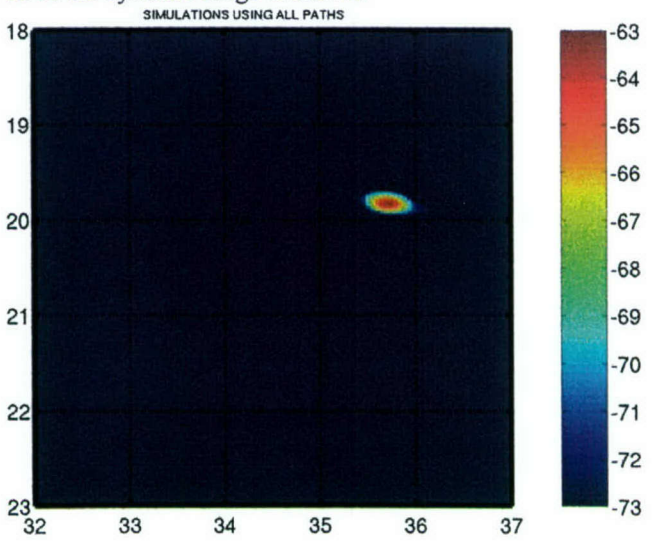

Figure 8. SAS image derived from the synthetic data shown in Fig. 5. A 10 dB dynamic range is shown, with real and synthetic data separated by a calibration offset.

4. SUMMARY AND CONCLUSIONS

This report summarizes a modeling effort geared towards evaluating the performance envelope of long-range SAS when sea surface forward scattering and reflection is utilized as the propagation channel. The effort was linked with a set of measurements performed by Kevin Williams (APL-UW) to examine SAS processing of a near-surface target, at range ~35 m, using an FM waveform for the transmit pulse.

Both the field and model data show that:

1. Four paths deliver the FM waveform roundtrip, one being the direct path to and from the target, and the other three involve interaction with the sea surface. Since two of these three paths are reciprocal, the result gives three time horizons.
2. The middle time horizon is the most energetic owing to the contribution of two paths.
3. The middle and third time horizons do not focus in SAS processing owing to interaction with sea surface for which the coherence time τ^* has been exceeded.

A key time scale for SAS processing involving the sea surface is the sea surface forward scattering coherence time, τ^*. From numerical studies [4], we take

$$\tau^* \approx \frac{3U}{gkH} \quad (1)$$

where k is acoustic wave number, U is wind speed (m/s), H is rms waveheight (m), and g is gravitational constant. Based on the center frequency of the FM pulse (8 kHz), and nominal rms waveheight (H = 14 cm), and wind speed (5 m/s), Eq. (1) puts $\tau^* \approx 0.3$ s, which is less than the pulse repetition period $\tau_{rep} = 0.5$ s. This implies that SAS processing for this kind of measurement scenario (i.e., interaction with the sea surface, with $\tau_{rep} > \tau^*$) effectively eliminates, or filters out, multipaths that involve the sea surface. The SAS image of a near-surface target collected under these conditions is based solely on the direct path, even though the second time horizon, involving coherent superposition of two paths sea-surface bounce paths, results in a more energetic return as seen in Fig. 6.

A second important time scale is $\frac{R_n}{c} \approx 0.025$ s, where R_n is the slant range for the nth ping. Since this scale is much less than τ^*, it is reasonable to assume that the sea surface was effectively "frozen" for the round trip.

An important role of the modeling effort from this work was to generate simulated data consistent with these two time scales. With the simulated data, the SAS processing could be done on the direct path alone, or any other another combination of the multipaths.

Sea surface interaction will invariably play a role in SAS methodologies whenever they are applied to: (1) long-range applications, e.g., over-the-horizon SAS (OTHSAS), or SAS Systems at Far Ranges and Severe Sites (SASSAFRASS), and (2) applications involving detection and imaging of near-surface targets.

For the "long range" application the sea surface forward scattering coherence time, τ^*, cannot be exceeded, if focusing of paths involving the sea surface is desired. For the "near-surface targets" application the same applies. However, it is also advantageous to use SAS measurement parameters that deliberately exceed τ^*, in order to filter out multipaths involving the sea surface. This results in better resolution and removal of spurious "ghost" images, and would find application in swimmer detection and other port security imaging tasks.

5. REFERENCES

[1] Williams K. L., Light R. D. , Miller V. W. and Kenney M. F. , "Bottom mounted rail system for Synthetic Aperture Sonar (SAS) imaging and acoustic scattering strength measurements: Design/operation/preliminary results," *Proceedings of the International Conference "Underwater Acoustic Measurements: Technologies and Results,"* Heraklion, Crete, Greece, 28 June – 1 July, 2005.

[2] P. H. Dahl and G. Kapodistrias, "Scattering from a single bubble near a roughened air-water interface: Laboratory measurements and modeling", *J. Acoust. Soc. Am.* **113**, pp 94-101, 2003.

[3] P. H. Dahl, "On bistatic sea surface scattering: Field measurements and modeling," *J. Acoust. Soc. Am.* **105**, pp 2155-2169, 1999.

[4] D. R. Dowling and D. R. Jackson, "Coherence of acoustic scattering from a dynamic rough surface," *J. Acoust. Soc. Am.* **93**, pp 3149-3157, 1993.

6. ACKNOWLEDGMENTS

The author thanks Dr. Kevin Williams (APL-UW) for making the SAS measurements and for producing the SAS images.